

1 **Transboundary and local air pollutants in western Japan**
2 **distinguished on the basis of ratios of metallic elements in size-**
3 **segregated aerosols**

4
5 **Yuta Taniguchi¹, Kojiro Shimada², Akinori Takami³, Neng-Huei Lin^{2,4}, Chak**
6 **K. Chan⁵, Yong Pyo Kim^{2,6}, Shiro Hatakeyama^{1,2,7*}**

7
8 ¹*Graduate School of Agriculture, Tokyo University of Agriculture and Technology, Fuchu, Tokyo*
9 ^{183-8509, Japan}

10 ²*Global Innovation Research Organization, Tokyo University of Agriculture and Technology,*
11 ^{Fuchu, Tokyo 183-8538, Japan}

12 ³*National Institute for Environmental Studies, Tsukuba, Ibaraki 305-0053, Japan*

13 ⁴*Department of Atmospheric Science and Department of Chemistry, National Central University,*
14 ^{Chung-Li, Taoyuan 32001, Taiwan}

15 ⁵*School of Energy and Environment, City University of Hong Kong, Hong Kong, China*

16 ⁶*Department of Chemical Engineering & Materials Science and Department of Environmental*
17 ^{Science & Engineering, Ewha Womans University, Seoul 03760, Republic of Korea}

18 ⁷*Center for Environmental Science in Saitama, Kazo 347-0115, Saitama, Japan*

19
20
21
22
23
24
25
26
27
28
29
30
31
32

32 *Corresponding author.

33 Tel: +81-480-73-8331 Fax: +81-480-70-2031

34 E-mail address: hatashir@cc.tuat.ac.jp

36 **ABSTRACT**

37

38 Trace metals in aerosols were observed at an urban site (Kumamoto, Kyushu, Japan) and a rural
39 site (Cape Hedo, Okinawa, Japan) to investigate the relative contributions of transboundary air
40 pollutants from mainland Asia and local air pollutants in western Japan. We used a cascade
41 impactor to collect aerosols in five size classes. We apportioned the sources of the air masses on
42 the basis of elemental components. Transboundary and local air pollutants were distinguished by
43 use of the Pb/Cu and V/As ratios in selected size fractions of aerosols. The contribution of Pb
44 (primarily from coal combustion in China) to total anthropogenic elements was greatest in spring,
45 autumn, and winter in the 0.5–1 μm size fraction at both collection sites. The atmospheric
46 environment at both sites was affected by this transboundary air pollutant. The contribution of Cu
47 (primarily from local vehicle traffic) to total anthropogenic elements was greatest in all seasons in
48 the 2.5–10 μm fraction at Kumamoto. Local air pollutants such as road dust, automobile brake
49 abrasion, and waste incineration affected ambient air quality in Kumamoto. Because these
50 pollutants resided mainly in the coarse aerosol fraction ($>2.5 \mu\text{m}$), most of them were not
51 transported to Cape Hedo in air bodies that we were able to trace to Kumamoto by backward
52 projection. Based on our data the ambient air quality at Cape Hedo was little affected by local air
53 pollutants emitted in the Kumamoto area.

54

55 Keywords: Size-segregated aerosol analysis; Chemical composition of metallic elements;
56 Difference in transboundary and local pollution; Elemental ratios.

57

58

59

60

61

62

63

64

65

66

67 INTRODUCTION

68

69 Severe air pollution has been caused by rapid economic growth in Asia (Chan and Yao, 2008,
70 Deng *et al.*, 2012). Emissions of gaseous pollutants and particulate matter (PM) from both
71 industries and residents have increased in this area (Ohara *et al.*, 2007), while the emission of
72 SO₂ and NO_x in China have decreased since 2006 and 2011, respectively (Xia *et al.*, 2016). PM is
73 transported from East Asian countries to Japan and Korea with prevailing westerly winds in the
74 winter and spring (Kaneyasu and Takada, 2004; Kim *et al.*, 2009, Itahashi *et al.*, 2010;
75 Hatakeyama *et al.*, 2014). Many studies have reported on the occurrence of transboundary air
76 pollution in western Japan (Kaneyasu *et al.*, 2014). Coal combustion is a major source of fine
77 particulate matter (PM) in China (Han *et al.*, 2005). Concentrations of PM smaller than 2.5 μm
78 (PM_{2.5}) derived from coal combustion are highest during the winter heating period in China.
79 PM_{2.5} has significant impacts on climate and human health (Shaheen *et al.*, 2005).

80 Toxic trace elements are often contained in PM (Shah *et al.*, 2006). In PM_{2.5}, these can cause
81 lung and cardiopulmonary injuries in humans (Shaheen *et al.*, 2005, IARC, 2012). The
82 concentrations and size distributions of trace elements in PM are mainly governed by the natural
83 and anthropogenic emission sources in the atmosphere (Samara and Voutsas, 2005). Major natural
84 emission sources are sea salt, soils, and forest fires. Major anthropogenic emission sources are
85 fuel combustion, waste incineration, and road traffic. In particular, traffic emissions consist of
86 various sources such as combustion products from fuel and lubricating oil, abrasion products
87 from brake pads and tires, and resuspension of road dust (El-Fadel and Hashisho, 2001).

88 The objective of this study was to determine the contribution of transboundary air pollution
89 transported from China to western Japan. In order to investigate the contributions of
90 transboundary air pollutants and local air pollutants in western Japan, we conducted observations
91 simultaneously at an urban site and a remote site, more than 1500 km southeast of Beijing. The
92 urban site was at Kumamoto University in Kumamoto City, on Kyushu Island, and the remote
93 site was the Cape Hedo Atmosphere and Aerosol Monitoring Station (CHAAMS) on Okinawa
94 Island. Takami *et al.* (2007) reported that the ambient air quality at Cape Hedo is influenced by
95 air pollutants transported by the northwest winter monsoon and the prevailing westerlies.

96 Cape Hedo usually receives air masses directly transported from eastern China, which pass
97 over the East China Sea. At times air masses from China that pass over the city of Kumamoto and
98 its vicinity are affected by locally emitted air pollutants on their way to Cape Hedo (Tatsuta,
99 2017).

100 This study focused on distinguishing between local pollutants and pollutants transported across
101 national boundaries. This was done by conducted measurements of toxic metallic elements in
102 different aerosol size fractions with four objectives: (1) to evaluate seasonal variation of trace
103 elements at Kumamoto and Cape Hedo; (2) to evaluate the size distribution of anthropogenic

104 trace elements in aerosols at the two sites; (3) to use of elemental ratios to determine the
105 contribution of transboundary and local air pollutants at both sites; and (4) to compare the
106 elemental compositions of aerosols transported directly to Cape Hedo from China and aerosols
107 transported to Cape Hedo from China by way of Kumamoto.

108

109 **METHODS**

110

111 ***Observations***

112 Sampling at Kumamoto City was conducted at the top of a nine-story building (32.81°N,
113 130.73°E) in Kumamoto University. Kumamoto is a city of 740,000 inhabitants on Kyushu
114 Island in western Japan, approximately 1500 km southeast of Beijing (Fig. 1). The city contains
115 no heavy industries; however, the sampling site was adjacent to a central arterial road with heavy
116 traffic. Furthermore, the location is in the eastern part of the city. We collected a total of 38 daily
117 samples during spring (13–17 March 2015 and 1–7 March 2016), summer (27 July to 2 August
118 2015), fall (14–21 October 2014 and 26–31 October 2015) and winter (17–21 December, 2014).

119 In Okinawa, sampling was conducted at CHAAMS (26.87°N, 128.25°E; 60 m above sea level),
120 located at the northern end of Okinawa Island, approximately 100 km north of Naha, the largest
121 city on the island, and approximately 1800 km southeast of Beijing (Fig. 1; details of the station
122 are reported in Takami *et al.*, 2007). There are no large industrial or residential areas nearby. Air
123 masses reaching Cape Hedo are transported from China, Korea, Japan, Southeast Asia, or the
124 Pacific Ocean, depending on weather conditions. We collected a total of 33 daily samples during
125 spring (13–17 April 2014 and 12–16 March 2015), fall (17–21 October 2014 and 26 October to 7
126 November 2015) and winter (13–17 December 2013).

127 Sampling was carried out by a five-stage cascade impactor (Nanosampler Model 3180,
128 Kanomax, Japan) operated with 40 L min⁻¹ air flow at 1 atm air pressure (Otani *et al.*, 2007).
129 Each sample was collected for 24 h from 10:00 am to 10:00 am the next day. Aerosols of particle
130 diameter (D_p) > 10 μm , 10 > D_p > 2.5 μm , 2.5 > D_p > 1 μm , 1 > D_p > 0.5 μm and 0.5 μm > D_p
131 were collected on PTFE filters 55 mm in diameter (PF020, Advantec, Japan). After sampling,
132 filters were cut into two pieces for analyses of trace metal elements and ionic components.

133

134 ***Size-Segregated Aerosol Analysis***

135 The metallic elements in the aerosol samples were quantitatively analyzed after digestion of
136 the samples with a mixture of 1.5 mL hydrofluoric acid, 2.5 mL nitric acid, and 0.5 mL hydrogen
137 peroxide in a Teflon vessel in a microwave oven operated at 200 W for 10 min. After digestion,
138 the hydrofluoric acid was removed by evaporation at 200°C on a hot plate in a hood. Sample
139 solutions were prepared by the addition of nitric acid solution and filtration. The atomic species
140 ²³Na, ²⁴Mg, ²⁷Al, ³⁹K, ⁵¹V, ⁵⁵Mn, ⁵⁷Fe, ⁶³Cu, ⁷⁵As, ⁸²Se, ⁸⁸Sr, ¹¹¹Cd, ¹²¹Sb, ¹³⁷Ba, ²⁰⁸Pb and ²⁰⁹Bi

141 were analyzed by inductively coupled plasma mass spectrometry (ICP-MS; Agilent 7500, Agilent
142 Technologies, USA).

143 Ionic components were measured by the method described in Tatsuta *et al.* (2017, this volume).
144

145 ***Backward-trajectory Analysis***

146 To identify the transport pathways of air masses, backward trajectories for 72 hours starting
147 from a height of 500 m above sea level were calculated using the HYSPLIT (HYbrid Single-
148 Particle Lagrangian Integrated Trajectory) model (Stein *et al.*, 2015) from the U.S. National
149 Oceanic and Atmospheric Administration (<http://ready.arl.noaa.gov/hypub-bin/trajtype.pl>) based
150 on GDAS (Global Data Assimilation System) global weather data by 1 degree.

151

152 **RESULTS AND DISCUSSION**

153

154 ***Source Identification of Metallic Elements Based on Enrichment Factors***

155 To determine the extent to which aerosols were emitted from natural or anthropogenic sources,
156 enrichment factors (EFs) for elements in each aerosol size fraction were calculated (Tables S1
157 and S2). The sea salt enrichment factor ($EF_{\text{sea salt}}$) and the crustal enrichment factor (EF_{crust}) are
158 defined by

159

$$160 \quad EF(X)_{\text{sea salt}} = (X/\text{Na})_{\text{aerosol}} / (X/\text{Na})_{\text{sea salt}} \quad (1)$$

161

162 and

163

$$164 \quad EF(X)_{\text{crust}} = (X/\text{Al})_{\text{aerosol}} / (X/\text{Al})_{\text{crust}}, \quad (2)$$

165

166 respectively, where X is the target element. $EF < 10$ typifies mainly natural sources, and $EF >$
167 10 suggests strong enrichment from non-natural sources (Waheed *et al.*, 2011). In this study, we
168 assumed that all Na originated from sea salt and all Al originated from the crust. In these
169 equations, we used the average chemical profile of sea salt from Chester (2009) and of
170 continental crust from Taylor and McLennan (1995).

171 The average $EF_{\text{sea salt}}$ values for Mg in all size ranges at both sites were lower than 10,
172 indicating a source in sea salt. The average EF_{crust} values for Fe, Sr, and Ba in all size ranges at
173 both sites were lower than 10, indicating a crustal source. Average $EF_{\text{sea salt}}$ and EF_{crust} values
174 were much higher than 10 for Cu, As, Cd, Sb, Pb and Bi in all size ranges, indicating emission
175 from anthropogenic sources. Enrichment factors for K, V, Mn, and Se had mostly anthropogenic
176 values (>10) in fine particles ($<2.5 \mu\text{m}$), but mostly crustal values (<10) in coarse particles (>2.5
177 μm).

178 From the resulting EF values, we determined the proportional contributions to total elements
179 from sea salt, crustal, and anthropogenic sources (Fig. 2). Here, total elements mean the sum of
180 mass concentrations of 16 elements in all size fractions sampled in this study in each season. At
181 Kumamoto, sea salt, crustal, and anthropogenic sources accounted for roughly 45%, 45%, and
182 10% of total elements in aerosols in spring, autumn and winter, respectively; however, these
183 percentages were about 73%, 21%, and 6%, respectively, in summer (Fig. 2a). At Cape Hedo, sea
184 salt, crustal, and anthropogenic sources accounted for about 86%, 12%, and 2%, respectively, in
185 the three seasons we took samples (Fig. 2b).

186 The influence of sea salt at Cape Hedo was greater than at Kumamoto, because Cape Hedo is
187 surrounded by the sea. At Kumamoto, the contribution of sea salt sources was much greater in
188 summer than in other seasons. Backward-trajectory analyses for the days on which we took
189 samples showed clearly that most air masses in summer were transported to Kumamoto primarily
190 over the ocean (Fig. S1).

191 These results suggest that the contribution of natural sources to the total elements was
192 dominant at both sites. The annual average contribution of anthropogenic sources was small,
193 although it was greater at Kumamoto (8%) than at Cape Hedo (2%).

194

195 ***Seasonal Variation of Anthropogenic Trace Elements***

196 Total concentrations of eight elements (V, Cu, Cd, As, Se, Sb, Pb, and Bi) are shown for each
197 aerosol size class in Fig. 3. Their EF values show that all of these elements, except V and Se,
198 were derived from anthropogenic sources in all size ranges at both sites (Table S1 and S2).
199 Concentrations were higher at Kumamoto than at Cape Hedo in all size ranges and seasons (Fig.
200 3). At both sites, the highest concentration was observed in the 0.5–1 μm fraction. At Cape Hedo,
201 the highest concentrations in the 0.5–1 μm , 1–2.5 μm , and 2.5–10 μm fraction were observed in
202 winter, indicating greater transboundary air pollutants in winter (Takami *et al.*, 2007).

203 As for anthropogenic sources, Waheed *et al.* (2011) attributed high metal concentrations in the
204 $D_p = 0.2\text{--}1 \mu\text{m}$ fraction of Shanghai aerosols to coal and fuel oil combustion. Other studies have
205 attributed high metal concentrations in the $D_p = 2\text{--}4 \mu\text{m}$ fraction at other localities to mechanical
206 abrasion of brake pads and tires (Gietl *et al.*, 2010; Oakes *et al.*, 2016). We show the proportions
207 of the eight anthropogenic elements at our sites in the 0.5–1 μm and 2.5–10 μm fractions for each
208 season in Fig. 4.

209 In the 0.5–1 μm fraction at both sites, Pb was the greatest contributor to total anthropogenic
210 elements in spring, autumn, and winter. Shimada *et al.* (2015) inferred that the source of Pb, As,
211 Se, and Cd in $\text{PM}_{2.5}$ at Cape Hedo may have been coal combustion in China on the basis of a
212 statistical analysis using positive matrix factorization. Tian *et al.* (2010, 2012) reported that trace
213 elements such as Pb, As, Se, and Cd in emissions from China were mainly derived from coal
214 combustion. Among these four elements, Cd made the smallest contribution to total

215 anthropogenic elements in spring, autumn, and winter at both sites, and As and Se were roughly
216 equal contributors at intermediate concentrations. In spring, autumn, and winter, most air masses
217 were transported to Kumamoto and Cape Hedo from China judging from back trajectories (Fig.
218 S1). The contributions of these four elements were in the order $Pb > As > Se > Cd$ at both sites in
219 these seasons. The contributions of those four elements are in the same order of volume in
220 emissions in China (Tian *et al.*, 2010, 2012). These results indicate that the anthropogenic
221 elements in 0.5–1 μm aerosols at Kumamoto and Cape Hedo were derived from coal combustion
222 in China.

223 In the 2.5–10 μm fraction at Kumamoto, Cu was the greatest contributor to total anthropogenic
224 elements in all seasons (Fig. 4a); however, this was not the case at Cape Hedo (Fig. 4b). This
225 indicates that Cu in the coarse particles was a local pollutant, mainly derived from abrasion of
226 vehicle brake pads (Sternbeck *et al.*, 2002).

227 The contribution of V to total anthropogenic elements in the 0.5–1 μm fraction was greatest in
228 summer at Kumamoto, where summer air masses were usually transported from the East China
229 Sea (Fig. S1). According to Eyring *et al.* (2010), the activity at large Chinese ports creates a very
230 high density of shipping traffic in the East China Sea, and Celio *et al.* (2015) reported that V in
231 fine particles is a tracer of fuel oil combustion. Thus, fuel oil combustion in ships appears to have
232 affected the summer air quality in Kumamoto. Likewise, ship emissions have been shown to
233 account for V in aerosols measured at Fukue Island, west of Kumamoto, and at Cape Hedo
234 (Shimada *et al.*, 2016).

235

236 ***Identification of Transboundary and Local Air Pollutants based on Metallic Element Ratios***

237 The next task was to characterize air sources on the basis of ratios of metal concentrations in
238 aerosols. We evaluated two ratios: Pb/Cu and V/As .

239 The Pb/Cu ratio was used as a means of identifying transboundary air pollution, using the Pb
240 concentration in the fine (0.5–1 μm) fraction and Cu in the coarse (2.5–10 μm) fraction. Coal
241 combustion in China is the predominant source of Pb in aerosols. Annual coal consumption in
242 China increased by 2.4 times from 2000 to 2010, at which time it amounted to 50% of worldwide
243 coal combustion (BP Statistical Review of World Energy, 2016). Coal combustion is the main
244 source of toxic elements such as Pb , Cd , As , and Se in aerosols. In particular, the concentration of
245 Pb emitted from coal combustion is larger than that of any other toxic element (Li *et al.*, 2012).
246 On the other hand, Fe , Ba , Cu , and Sb are derived from abrasion of vehicle brake pads and tires
247 (Hulskotte *et al.*, 2014). Among these, Fe and Ba are not suitable tracers of vehicle-brake
248 abrasion, because they are also abundant in soil; therefore Cu was used a tracer of vehicle
249 abrasion at Kumamoto. Cu in coarse particles is emitted from abrasion of vehicle brakes
250 (Sternbeck *et al.*, 2002), whereas Cu in fine particles is derived from combustion (Font *et al.*,
251 2015). Cu concentrations in the coarse size range were considerably higher at Kumamoto than at

252 | Cape Hedo, because Kumamoto had much more vehicle traffic. Furthermore, because PM₁₀ has a
253 much shorter residence time in the atmosphere than PM_{2.5} (Shin *et al.*, 2009), we can expect that
254 little or no Cu in coarse particles emitted in Kumamoto reached Cape Hedo.

255 The size distribution of Cu concentrations at Kumamoto differed from that at Cape Hedo (Fig.
256 5b). At Kumamoto, Cu concentrations were highest in the coarse fraction owing to the
257 contribution of vehicle abrasion in Kumamoto. At Cape Hedo, Cu concentrations were lowest in
258 the coarse fraction and highest in the fine fraction. We attributed this difference to the more rapid
259 deposition of coarse particles than fine particles during long-range transport (Allen *et al.*, 2001).

260 Pb/Cu ratios were higher in all seasons at Cape Hedo (Fig. S2a). The ratio in winter was
261 particularly high at both sites. Similar to the results of Shimada *et al.* (2014), the contribution of
262 coal combustion at Cape Hedo is greater in winter than in other seasons. V/As ratios were also
263 used as a means of distinguishing among transboundary pollutants. Fuel oil combustion releases
264 V in aerosols (Viana *et al.*, 2014), and concentrations of V are often used as a tracer of ship
265 emissions. Coal combustion releases As (Tian *et al.*, 2010), and almost all As observed in
266 western Japan originates from China (Sakata *et al.*, 2014) as coal is little used in Japan. Therefore
267 the V/As ratio should effectively distinguish ship emissions from coal emissions. Because
268 particles derived from fossil fuel combustion dominate the 0.2–1 μm aerosol fraction (Waheed *et al.*
269 *et al.*, 2011), we used the elemental concentrations of the 0.5–1 μm fraction to determine V/As (Fig.
270 S2b).

271 The V/As ratio at Kumamoto was particularly high in summer (Fig. S2b), when air masses are
272 transported to Kumamoto from the East China Sea (Fig. S1), indicating large contributions of V
273 from ship emissions. The ratio was low at both sites in spring, autumn, and winter, but was
274 particularly low in winter. This is attributed to the large contribution of As from coal combustion
275 in China, because air masses reaching Kumamoto in winter were largely derived from China (Fig.
276 S1).

277 278 ***Comparisons of Aerosols in the Same Air Masses at Kumamoto and Cape Hedo***

279 In two cases, backward-trajectory analysis showed that the same air mass was observed at both
280 Kumamoto and Cape Hedo (Fig. S3). The air mass reaching Cape Hedo on 17 October 2014
281 passed over Kumamoto on 16 October, and the air mass reaching Cape Hedo on 31 October 2015
282 passed over Kumamoto the same day. Fig. S4 compares the mass proportions of the 16 metallic
283 elements in coarse particles at our two measurement sites. The correlation between sites was very
284 strong ($r^2 = 0.97$, $p < 0.05$), and the regression-line slope was 0.93. That most of the elements
285 plotted on the 1:1 line indicated that they did not increase or decrease during transport from
286 Kumamoto to Cape Hedo. However, percentages of Cu, Sb, and K departed greatly from the 1:1
287 line, with Cu and Sb being higher at Kumamoto and K being higher at Cape Hedo.

288 Looking in detail at Sb (Fig. 5a) and Cu (Fig. 5b), we found the highest concentrations in the
289 0.5–1 μm fraction at Cape Hedo, but at Kumamoto, Cu had its peak concentration in the 2.5–10
290 μm fraction, and Sb had a bimodal distribution, with peaks in the 0.5–1 μm and 2.5–10 μm
291 fractions. Sb and Cu are found in coarse particles emitted from the abrasion of vehicle brakes
292 (Hulskotte *et al.*, 2014), as brake pads contain 1–5% Sb_2S_3 (Varrica *et al.*, 2013), and brake
293 linings contain Cu (Sternbeck *et al.*, 2002). Furthermore, particles produced by mechanical
294 abrasion are mainly in the 2–4 μm size range (Gietl *et al.*, 2010). According to Pio *et al.* (2013),
295 Cu/Sb ratios in material derived from vehicle abrasion range from 7.1 to 12.1, and in our results
296 the annual average Cu/Sb ratio at Kumamoto was in the same range (10.3). The sum of the
297 evidence indicates that Cu and Sb are enriched in coarse aerosols at Kumamoto that settle out
298 from air bodies before reaching Cape Hedo.

299 Conversely, the content ratio of K at Kumamoto was smaller than at Cape Hedo (Fig. S4),
300 meaning that the K content in fine particles was larger at Kumamoto than at Cape Hedo.
301 Concentrations of K were highest in the coarse (2.5–10 μm) fraction at both sites (Fig. 5c). Our
302 analysis of EF values showed that particles in this size range originated from sea salt or soil dust
303 (Table S1 and S2). Because the concentration of K in coarse particles was higher at Cape Hedo
304 than at Kumamoto, some addition of K must have occurred during transport, presumably from
305 sea salt. On the other hand, K concentrations were also high in the 0.5–1 μm fraction at
306 Kumamoto. Waste incineration (Oakes *et al.*, 2016) and biomass burning (Chen *et al.*, 2013) are
307 known generators of high K concentrations in fine aerosols. We attributed the K content in fine
308 aerosols from Kumamoto to this cause.

309 Chloride is also emitted from waste incineration and biomass burning (Kaneyasu *et al.*, 1999).
310 The correlation of Cl^- and K concentrations in fine aerosols was poor ($r^2 = 0.0038$) at Cape Hedo,
311 but was appreciable at Kumamoto ($r^2 = 0.82$, $p < 0.05$); we therefore attributed both K and Cl^- in
312 fine aerosols at Kumamoto to emissions from waste incineration or biomass burning (Fig. 6a, 6b).
313 We determined the correlation between Na^+ and Cl^- concentrations in coarse particles (Fig. 6c, 6d)
314 and fine particles (Fig. 6e, 6f) at Kumamoto and Cape Hedo during the observation period. As
315 expected, Na^+ in both size ranges originated from sea salt. As for Cl^- , the correlation was good at
316 both sites in the coarse particle size range, consistent with sea salt, but the correlation was poor at
317 both sites in the fine particles (Fig. 6e, 6f). Furthermore, the average concentrations of Cl^- in fine
318 particles were higher at Kumamoto (0.91 neq/m^3) than at Cape Hedo (0.14 neq/m^3). It appears
319 that local emissions such as waste incineration or biomass burning contributed more to the
320 ambient air quality in Kumamoto than at Cape Hedo.

321 In sum, our results showed that Cu and Sb in coarse aerosols can be tracers of local emissions
322 from vehicle brakes and tires, and K in fine aerosols can be a tracer of local emissions from waste
323 incineration or biomass burning.

324

325 CONCLUSIONS

326

327 At the Kumamoto site, local air pollutants, including elements derived from abrasion of vehicle
328 brakes, affected ambient air quality. However, because these pollutants resided mainly in coarse
329 aerosol particles, most of them were not transported long distances, and air quality at the Cape
330 Hedo site was relatively unaffected by them. This means that in air masses from China that arrive
331 at Cape Hedo after passing over Kumamoto, almost all trace elements in the fine aerosol particles
332 were from China. Our results show that the contribution of most anthropogenic elements in
333 transboundary air pollutants, particularly in fine particles, is greater than that of local air
334 pollutants at Kumamoto. Therefore, transboundary air pollutants are of special concern when
335 assessing the effects of ambient trace elements on human health in western Japan. Trace element
336 concentrations and their ratios, specifically Pb/Cu and V/As, are effective in distinguishing
337 transboundary air pollutants from local air pollutants. In particular, Cu and Sb are useful
338 indicators of local emissions from vehicle brake abrasion, and K is an indicator of local emissions
339 from waste incineration or biomass burning.

340

341 ACKNOWLEDGMENTS

342 This research was supported by the Global Environment Research Fund (5-1452 and 2-1403) of
343 the Ministry of the Environment of Japan.

344

345 REFERENCES

346

- 347 Allen, A. G., Nemitz, E., Shi, J. P., Harrison, R. M., and Greenwood, J. C. (2001). Size
348 distributions of trace metals in atmospheric aerosols in the United Kingdom. *Atmospheric*
349 *Environment*, 35(27), 4581-4591.
- 350 BP Statistical Review of World Energy. (2016). [http://www.bp.com/en/global/corporate/energy-](http://www.bp.com/en/global/corporate/energy-economics/statistical-review-of-world-energy.html)
351 [economics/statistical-review-of-world-energy.html](http://www.bp.com/en/global/corporate/energy-economics/statistical-review-of-world-energy.html)
- 352 Celo, V., Dabek-Zlotorzynska, E., and McCurdy, M. (2015). Chemical characterization of
353 exhaust emissions from selected Canadian Marine vessels: the case of trace metals and
354 lanthanoids. *Environmental science and technology*, 49(8), 5220-5226.
- 355 Chan, C. K., and Yao, X. (2008). Air pollution in mega cities in China. *Atmospheric Environment*,
356 42(1), 1-42.
- 357 Chen, S. C., Hsu, S. C., Tsai, C. J., Chou, C. C. K., Lin, N. H., Lee, C. T., Roam, G.D., and Pui,
358 D. Y. (2013). Dynamic variations of ultrafine, fine and coarse particles at the Lu-Lin
359 background site in East Asia. *Atmospheric Environment*, 78, 154-162.
- 360 Chester, R. (2009). *Marine Geochemistry*, Wiley-Blackwell, pp5236.

- 361 Deng, J., Du, K., Wang, K., Yuan, C. S. and Zhao, J. (2012). Long-term atmospheric visibility
362 trend in Southeast China, 1973–2010. *Atmos. Environ.* 59: 11–21.
- 363 El-Fadel, M., and Hashisho, Z. (2001). Vehicular emissions in roadway tunnels: a critical review.
364 *Critical Reviews in Environmental Science and Technology*, 31(2), 125-174.
- 365 Eyring, V., Isaksen, I. S., Berntsen, T., Collins, W. J., Corbett, J. J., Endresen, O., Grainger, R.G.,
366 Moldanova, J., Schlager, H., and Stevenson, D. S. (2010). Transport impacts on atmosphere
367 and climate: Shipping. *Atmospheric Environment*, 44(37), 4735-4771.
- 368 Font, A., de Hoogh, K., Leal-Sanchez, M., Ashworth, D. C., Brown, R. J., Hansell, A. L., and
369 Fuller, G. W. (2015). Using metal ratios to detect emissions from municipal waste
370 incinerators in ambient air pollution data. *Atmospheric Environment*, 113, 177-186.
- 371 Gietl, J. K., Lawrence, R., Thorpe, A. J., and Harrison, R. M. (2010). Identification of brake wear
372 particles and derivation of a quantitative tracer for brake dust at a major road. *Atmospheric*
373 *Environment*, 44(2), 141-146.
- 374 Han, L., Zhuang, G., Sun, Y., and Wang, Z. (2005). Local and non-local sources of airborne
375 particulate pollution at Beijing. *Science in China Series B: Chemistry*, 48(3), 253-264.
- 376 Hatakeyama, S., Ikeda, K., Hanaoka, S., Watanabe, I., Arakaki, T., Bandow, H., Sadanaga, Y.,
377 Kato, S., Kajii, Y. Zhang, D., Okuyama, K., Ogi, T. Fujimoto, T. Seto, T., Shimizu, A.,
378 Sugimoto, N. and Takami, A. (2014). Aerial observations of air masses transported from
379 East Asia to the Western Pacific: Vertical structure of polluted air masses, *Atmos. Environ.*,
380 97: 456–461.
- 381 Hulskotte, J. H. J., Roskam, G. D., and Van Der Gon, H. D. (2014). Elemental composition of
382 current automotive braking materials and derived air emission factors. *Atmospheric*
383 *Environment*, 99, 436-445.
- 384 IARC (2012). ARSENIC, METALS, FIBRES, AND DUSTS, A review of human carcinogens.
385 IARC monographs on the evaluation of carcinogenic risks to humans.
386 (<http://monographs.iarc.fr/ENG/Monographs/vol100C/mono100C.pdf> Accessed 7 Mar. 2017)
- 387 Itahashi, S., Yumimoto, K., Uno, I., Eguchi, K., Takemura, T., Hara, Y., Shimizu, A., Sugimoto,
388 N. and Liu, Z. (2010). Structure of dust and air pollutant outflow over East Asia in the
389 spring, *Geophys. Res. Lett.*, 37: L20806.
- 390 Kaneyasu, N., and Takada, H. (2004). Seasonal variations of sulfate, carbonaceous species (black
391 carbon and polycyclic aromatic hydrocarbons), and trace elements in fine atmospheric
392 aerosols collected at subtropical islands in the East China Sea. *Journal of Geophysical*
393 *Research: Atmospheres*, 109(D6).
- 394 Kaneyasu, N., Yoshikado, H., Mizuno, T., Sakamoto, K., and Soufuku, M. (1999). Chemical
395 forms and sources of extremely high nitrate and chloride in winter aerosol pollution in the
396 Kanto Plain of Japan. *Atmospheric Environment*, 33(11), 1745-1756.

- 397 Kaneyasu, N., Yamamoto, S., Sato, K., Takami, A., Hayashi, M., Hara, K., Kawamoto, K.,
398 Okuda, T., and Hatakeyama, S. (2014). Impact of long-range transport of aerosols on the PM
399 2.5 composition at a major metropolitan area in the northern Kyushu area of Japan.
400 *Atmospheric Environment*, 97, 416-425.
- 401 Kim, K. H., Ma, C. J., and Okuda, T. (2009). An analysis of long-term changes in airborne toxic
402 metals in South Korea's two largest cities from 1991 to 2004. *Environmental Science and*
403 *Pollution Research*, 16(5), 565-572.
- 404 Li, Q., Cheng, H., Zhou, T., Lin, C., and Guo, S. (2012). The estimated atmospheric lead
405 emissions in China, 1990–2009. *Atmospheric Environment*, 60, 1-8.
- 406 Oakes, M. M., Burke, J. M., Norris, G. A., Kovalcik, K. D., Pancras, J. P., and Landis, M. S.
407 (2016). Near-road enhancement and solubility of fine and coarse particulate matter trace
408 elements near a major interstate in Detroit, Michigan. *Atmospheric Environment*, 145, 213-
409 224.
- 410 Ohara, T. A. H. K., Akimoto, H., Kurokawa, J. I., Horii, N., Yamaji, K., Yan, X., and Hayasaka,
411 T. (2007). An Asian emission inventory of anthropogenic emission sources for the period
412 1980–2020. *Atmospheric Chemistry and Physics*, 7(16), 4419-4444.
- 413 Otani, Y., Eryu, K., Furuuchi, M., Tajima, N., and Tekasakul P. (2007). Inertial Classification of
414 Nano particles with Fibrous Filters, *Aerosol and Air Quality Research*, 7, 343-352 .
- 415 Pio, C., Mirante, F., Oliveira, C., Matos, M., Caseiro, A., Oliveira, C., Querol, X., Alves, C.,
416 Martins, N., Cerqueira, M., Camoes, F., Silva, H., and Plana, F. (2013) Size-segregated
417 chemical composition of aerosol emissions in an urban road tunnel in Portugal. *Atmospheric*
418 *Environment*, 71, 15-25.
- 419 Sakata, M., Ishikawa, T., and Mitsunobu, S. (2014). Contribution of Asian outflow to
420 atmospheric concentrations of sulfate and trace elements in aerosols during winter in Japan.
421 *Geochemical Journal*, 48, 479-490.
- 422 Samara, C., and Voutsas, D. (2005). Size distribution of airborne particulate matter and associated
423 heavy metals in the roadside environment. *Chemosphere*, 59(8), 1197-1206.
- 424 Shah, M. H., Shaheen, N., Jaffar, M., Khaliq, A., Tariq, S. R., and Manzoor, S. (2006). Spatial
425 variations in selected metal contents and particle size distribution in an urban and rural
426 atmosphere of Islamabad, Pakistan. *Journal of Environmental Management*, 78(2), 128-137.
- 427 Shaheen, N., Shah, M. H., Khaliq, A., and Jaffar, M. (2005). Metal levels in airborne
428 particulate matter in urban Islamabad, Pakistan. *Bulletin of Environmental Contamination*
429 *and Toxicology*, 75(4), 739-746.
- 430 Shin, H.H., Burnett, R.T., Stieb, D.M., and Jessiman, B. (2009) Measuring health accountability
431 of air quality management. *Air Qual Atmos Health* 2:11–20
- 432 Shimada, K., Shimada, M., Takami, A., Hasegawa, S., Fushimi, A., Arakaki, T., Watanabe, I.,
433 and Hatakeyama, S. (2015). Mode and place of origin of carbonaceous aerosols transported

434 from East Asia to Cape Hedo, Okinawa, Japan. *Aerosol and Air Quality Research*. 15(3),
435 799-813.

436 Shimada, K., Araki, Y., Yoshino, A., Takami, A., Yang, X., Chen, X., Meng, F., and Hatakeyama,
437 S. (2016). Concentrations of metallic elements in long-range-transported aerosols measured
438 simultaneously at three coastal sites in China and Japan. *Journal of Atmospheric Chemistry*
439 (submitted).

440 Stein, A.F., Draxler, R.R., Rolph, G.D., Stunder, B.J.B., Cohen, M.D., and Ngan, F., (2015).
441 NOAA's HYSPLIT atmospheric transport and dispersion modeling system, *Bull. Amer.*
442 *Meteor. Soc.*, **96**, 2059-2077, <http://dx.doi.org/10.1175/BAMS-D-14-00110.1>

443 Sternbeck, J., Sjödin, Å., and Andréasson, K. (2002). Metal emissions from road traffic and the
444 influence of resuspension—results from two tunnel studies. *Atmospheric Environment*,
445 *36*(30), 4735-4744.

446 Takami, A., Miyoshi, T., Shimono, A., Kaneyasu, N., Kato, S., Kajii, Y., and Hatakeyama, S.
447 (2007). Transport of anthropogenic aerosols from Asia and subsequent chemical
448 transformation. *Journal of Geophysical Research: Atmospheres*, *112*(D22).

449 Tatsuta, S., Shimada, K., Chan, C. K., Kim, Y. P., Lin, N. H., Takami, A., and Hatakeyama, S.
450 (2017). Size-segregated analysis of ionic composition of aerosols transported from the East
451 Asia to Cape Hedo, Okinawa through Kumamoto city. *Aerosol Air Qual. Res., this issue*.

452 Taylor, S. R., and McLennan, S. M. (1995). The geochemical evolution of the continental crust.
453 *Reviews of Geophysics*, *33*(2), 241-265.

454 Tian, H., Cheng, K., Wang, Y., Zhao, D., Lu, L., Jia, W., and Hao, J. (2012). Temporal and
455 spatial variation characteristics of atmospheric emissions of Cd, Cr, and Pb from coal in
456 China. *Atmospheric Environment*, *50*, 157-163.

457 Tian, H. Z., Wang, Y., Xue, Z. G., Cheng, K., Qu, Y. P., Chai, F. H., and Hao, J. M. (2010).
458 Trend and characteristics of atmospheric emissions of Hg, As, and Se from coal combustion
459 in China, 1980–2007. *Atmospheric Chemistry and Physics*, *10*(23), 11905-11919.

460 Varrica, D., Bardelli, F., Dongarrà, G., and Tamburo, E. (2013). Speciation of Sb in airborne
461 particulate matter, vehicle brake linings, and brake pad wear residues. *Atmospheric*
462 *Environment*, *64*, 18-24.

463 Viana, M., Hammingh, P., Colette, A., Querol, X., Degraeuwe, B., de Vlieger, I., and van
464 Aardenne, J. (2014). Impact of maritime transport emissions on coastal air quality in Europe.
465 *Atmospheric Environment*, *90*, 96-105.

466 Waheed, A., Li, X., Tan, M., Bao, L., Liu, J., Zhang, Y., Zhang, G., and Li, Y. (2011). Size
467 distribution and sources of trace metals in ultrafine/fine/coarse airborne particles in the
468 atmosphere of Shanghai. *Aerosol Science and Technology*, *45*(2), 163-171.

469 Xia, Y., Zhao, Y. and Nielsen, C. P. (2016). Benefits of China's efforts in gaseous pollutant
470 control indicated by the bottom-up emissions and satellite observations 2000-2014. *Atmos.*
471 *Environ.*, 136: 43-53.

472

473

ACCEPTED MANUSCRIPT

474

Figure Captions

475 **Fig. 1.** The location of two observation sites: KM and HD.

476 **Fig. 2.** Average proportions of sea salt, soil, and anthropogenic sources in total metallic elements
477 for each season at Kumamoto (a) and Cape Hedo (b).

478 **Fig. 3.** Average concentrations of total anthropogenic metallic elements (V, Cu, As, Se, Cd, Sb,
479 Pb, Bi) by particle size in each season at Kumamoto (a) and Cape Hedo (b).

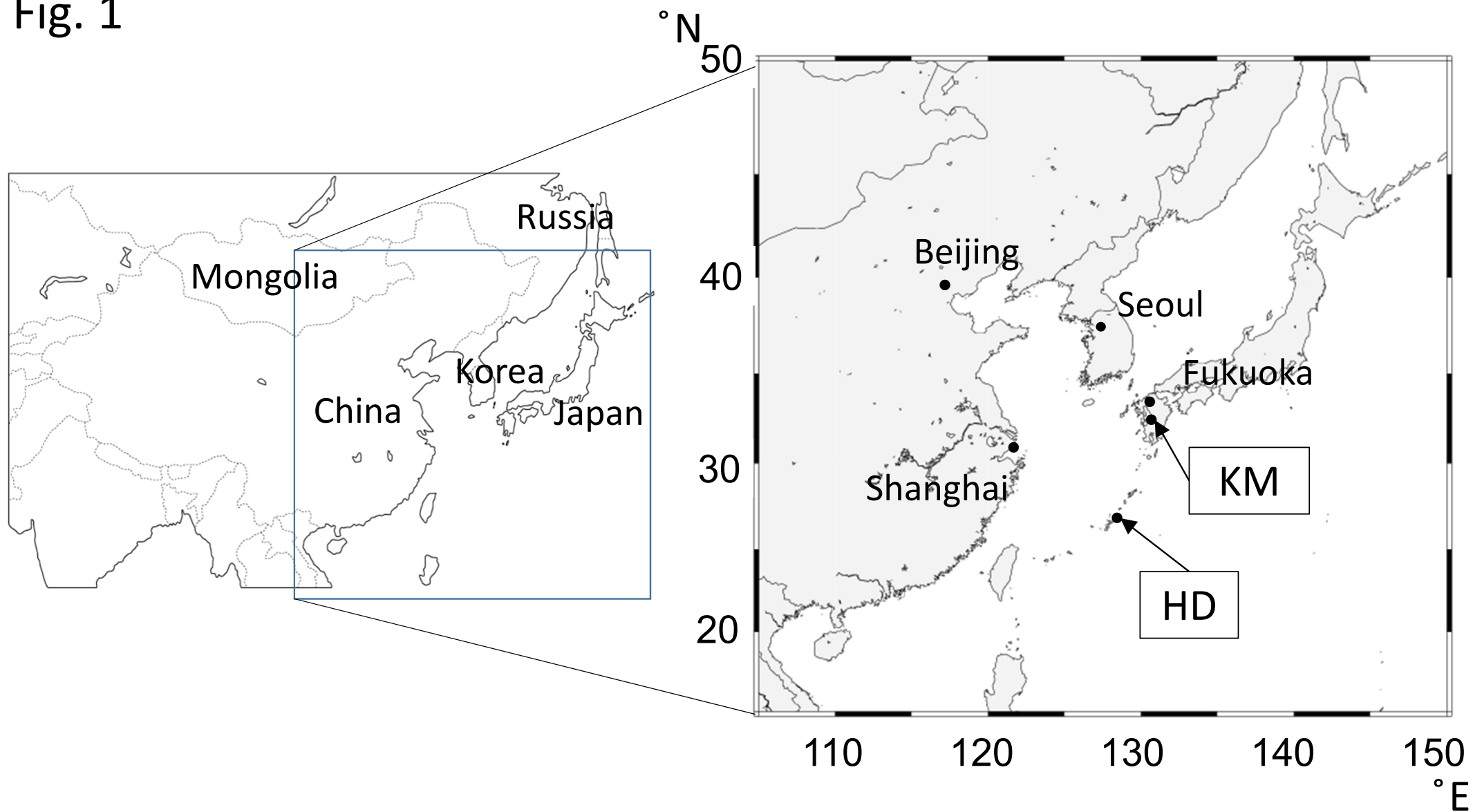
480 **Fig. 4.** Average chemical compositions of anthropogenic metallic elements (V, Cu, As, Se, Cd,
481 Sb, Pb, Bi) in the 0.5–1 μm and 2.5–10 μm size fractions in each season at Kumamoto (a) and
482 Cape Hedo (b).

483 **Fig. 5.** Average concentrations of Sb (a), Cu (b), and K (c) by particle size in the autumn
484 observation period at Kumamoto and Cape Hedo.

485 **Fig. 6.** Correlation between Cl^- and K in fine particles ($<2.5 \mu\text{m}$) at Kumamoto (a) and Cape
486 Hedo (b). Correlation between Na^+ and Cl^- in coarse particles ($>2.5 \mu\text{m}$) at Kumamoto (c) and
487 Cape Hedo (d). Correlation between Na^+ and Cl^- in fine particles ($<2.5 \mu\text{m}$) at Kumamoto (e) and
488 Cape Hedo (f).

489

Fig. 1



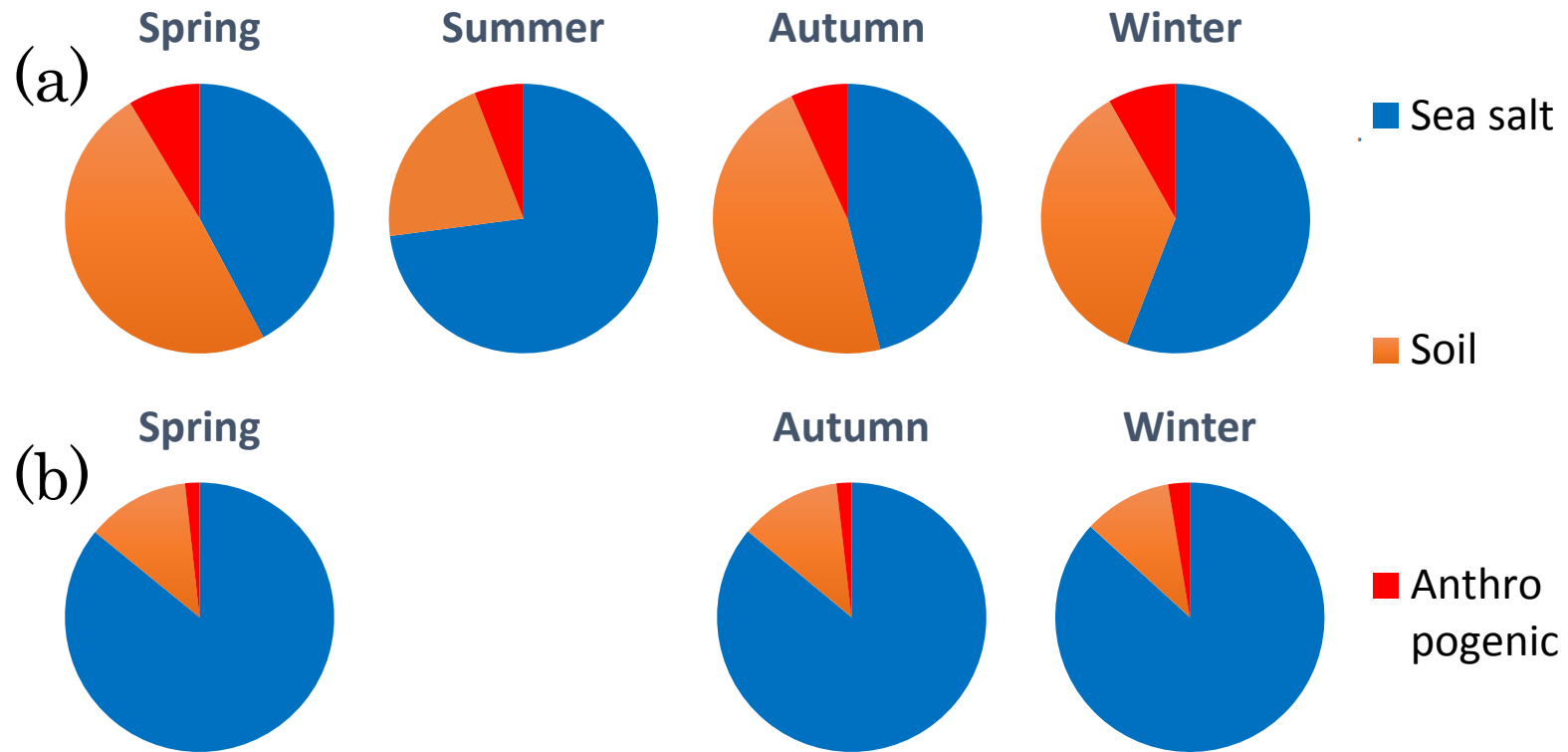


Fig. 2 (a) (b)

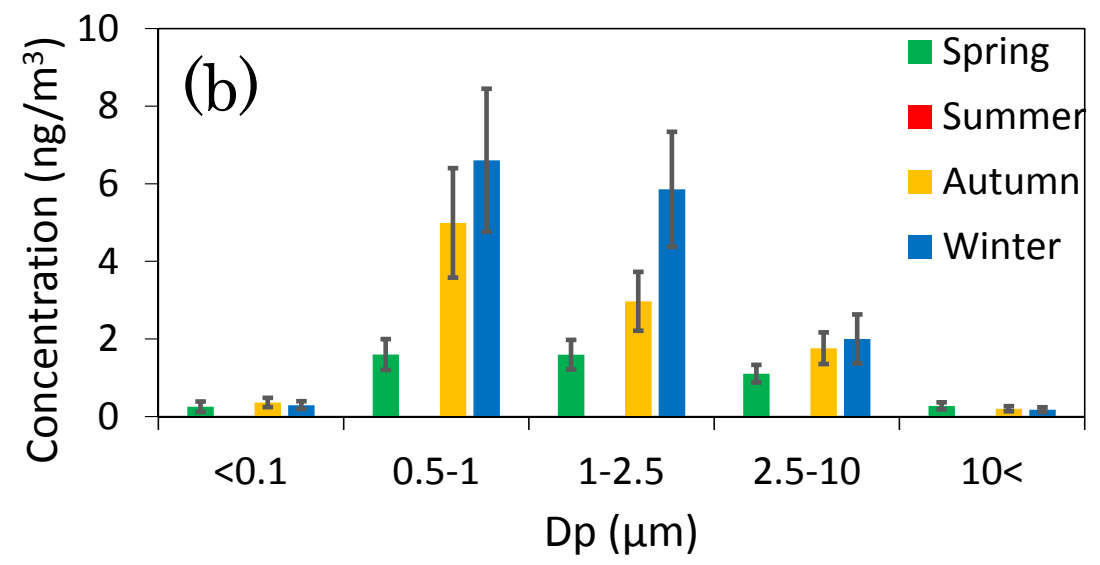
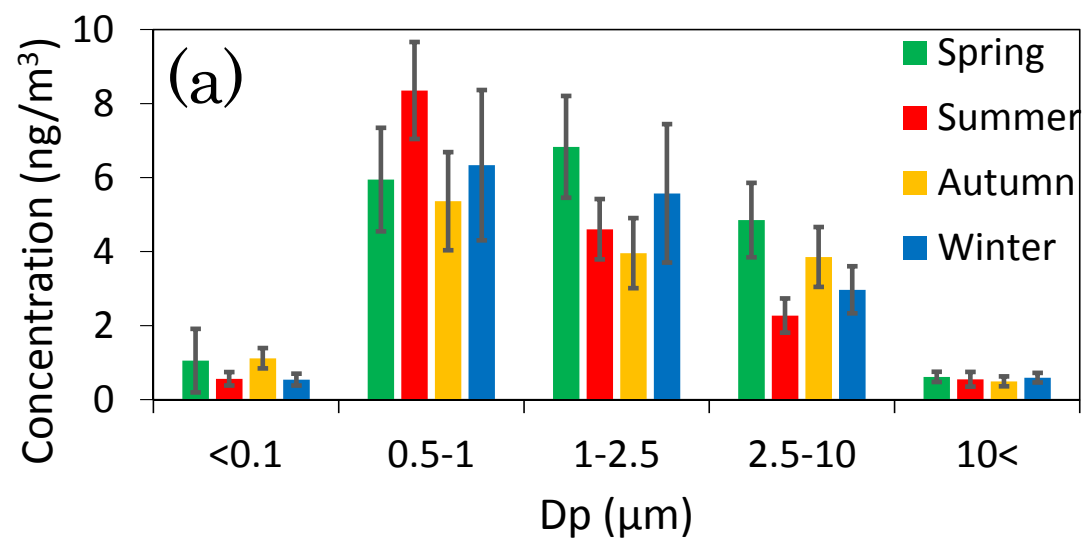


Fig. 3 (a) (b)

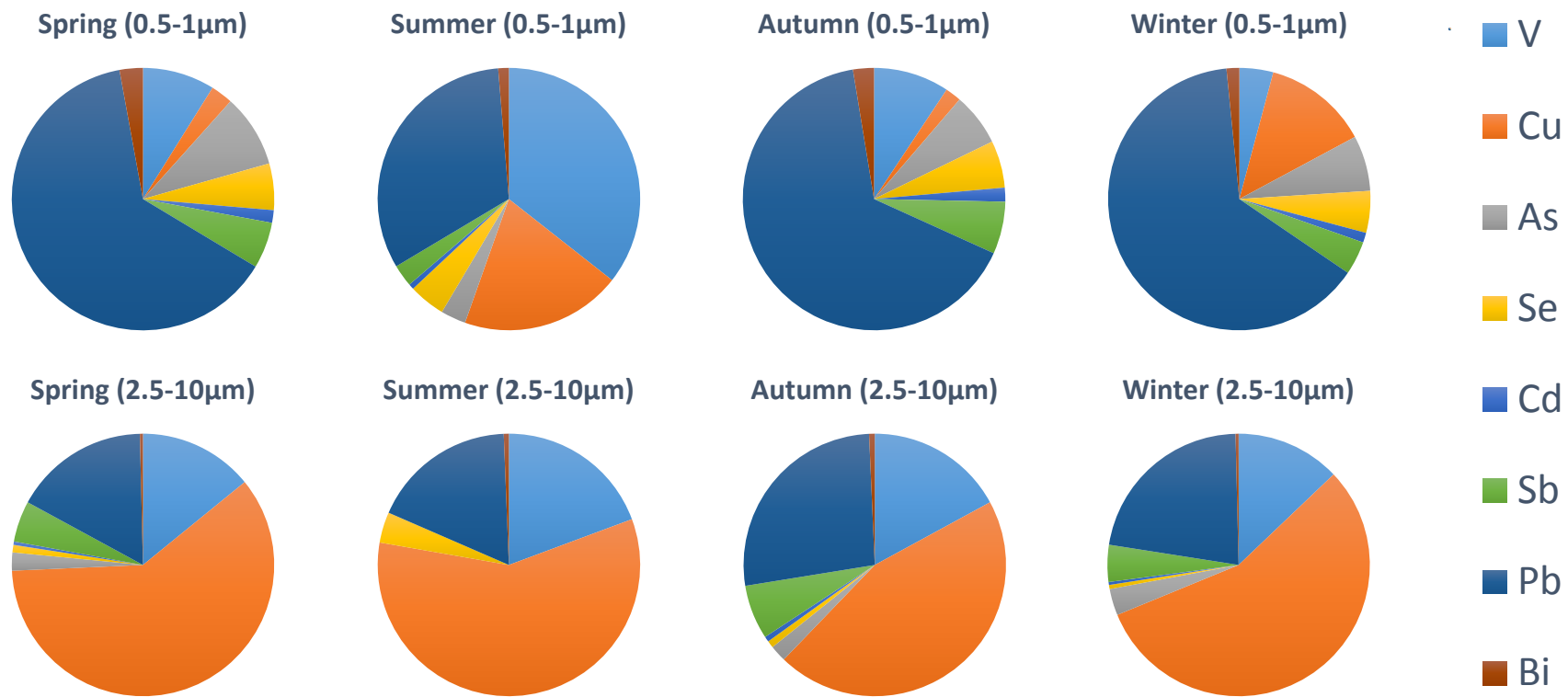


Fig. 4 (a)

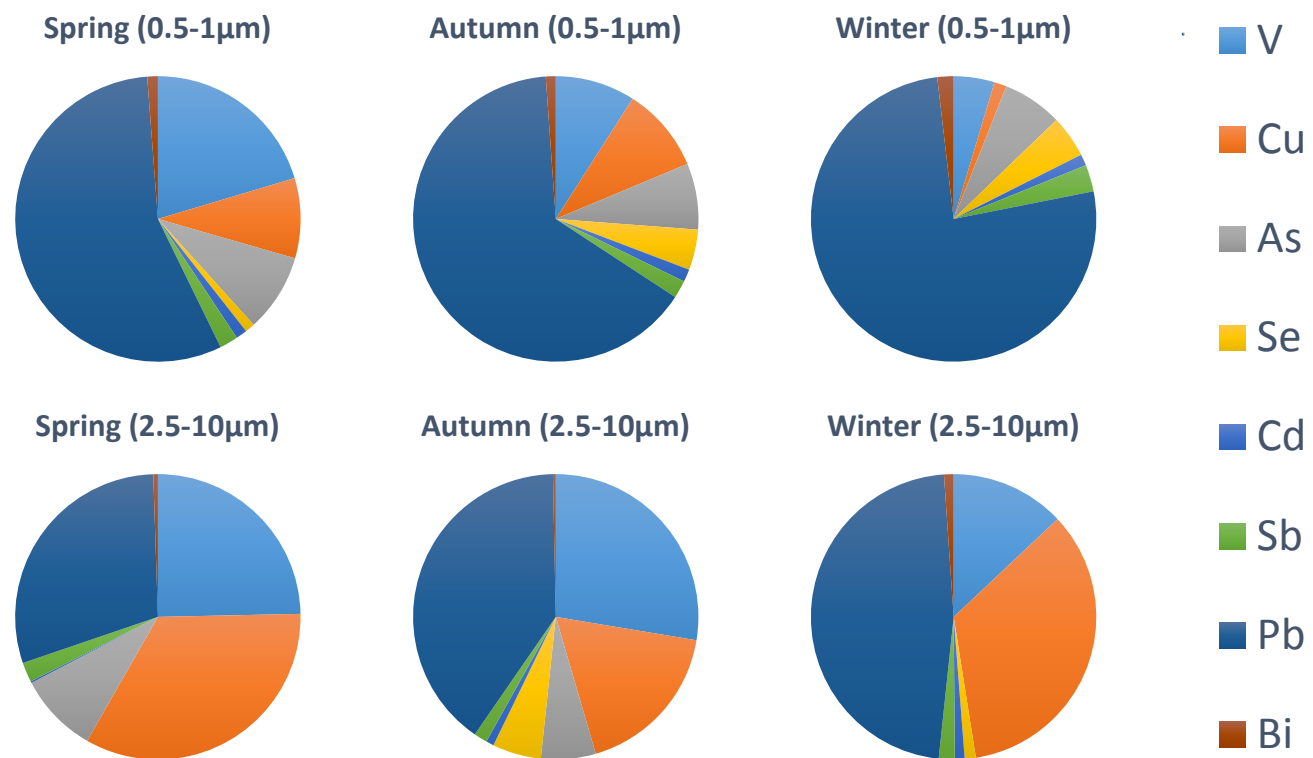


Fig. 4 (b)

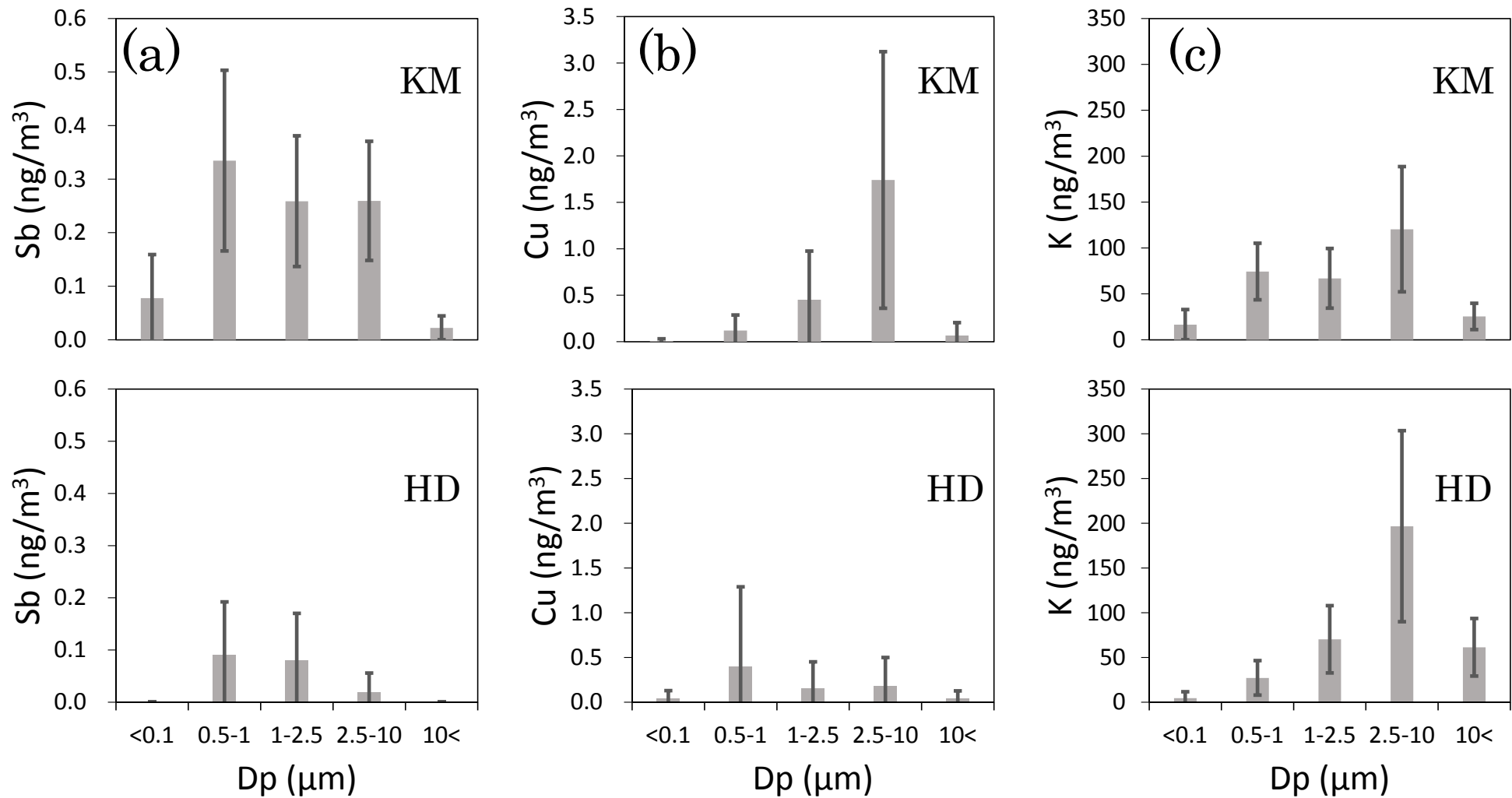


Fig. 5 (a)(b)(c)

